

Supplementary figure:

Fig. S1 shows the elemental mapping of the nanocrystalline $\text{Fe}_{85.2}\text{B}_{10}\text{P}_4\text{Cu}_{0.8}$ alloys at the region where the one α -Fe nanocrystal distributed. The seed element, Cu is randomly distributed. The P element is enriched in the adjacent amorphous phase, and on the other hand Fe element has a higher concentration in the crystalline phase (α -Fe nanocrystals).

Fig. S2 presents the collected data of the particle size and pore size the grain size of a-Fe nanocrystals (a, b) in as-annealed $\text{Fe}_{85.2}\text{B}_{14}\text{Cu}_{0.8}$ and $\text{Fe}_{85.2}\text{B}_{10}\text{P}_4\text{Cu}_{0.8}$ alloys and pore size (c, d) in as-dealloyed $\text{Fe}_{85.2}\text{B}_{14}\text{Cu}_{0.8}$ and $\text{Fe}_{85.2}\text{B}_{10}\text{P}_4\text{Cu}_{0.8}$ alloys. The value of D_2 and d_2 was obtained from the three TEM images similar with Figs. 2a, d and 4a, d for each condition. The data of D_2 and d_2 were obtained from more than 125 sites for each TEM image by using Nanomeasure® software. The distribution ratio of α -Fe nanocrystals in annealed $\text{Fe}_{85.2}\text{B}_{14}\text{Cu}_{0.8}$ alloys in Fig. S2 b and nanopores in dealloyed $\text{Fe}_{85.2}\text{B}_{10}\text{P}_4\text{Cu}_{0.8}$ alloys in Fig. S2 d is typical of the normal distribution. On the other hand, that of α -Fe nanocrystals in annealed $\text{Fe}_{85.2}\text{B}_{10}\text{P}_4\text{Cu}_{0.8}$ alloys in Fig. S2 a and nanopores in dealloyed $\text{Fe}_{85.2}\text{B}_{14}\text{Cu}_{0.8}$ alloys in Fig. S2 c shows a larger divergence, particular the α -Fe nanocrystals with a large size of more than 60 nm and nanopores with a pore size of larger than 30 nm. The data demonstrate that the uniformity of the nanoporous structure in dealloyed $\text{Fe}_{85.2}\text{B}_{10}\text{P}_4\text{Cu}_{0.8}$ alloys is better than that of dealloyed $\text{Fe}_{85.2}\text{B}_{10}\text{P}_4\text{Cu}_{0.8}$ alloys due to the worse microstructure of annealed $\text{Fe}_{85.2}\text{B}_{14}\text{Cu}_{0.8}$ alloys with irregular-shaped a-Fe particles.

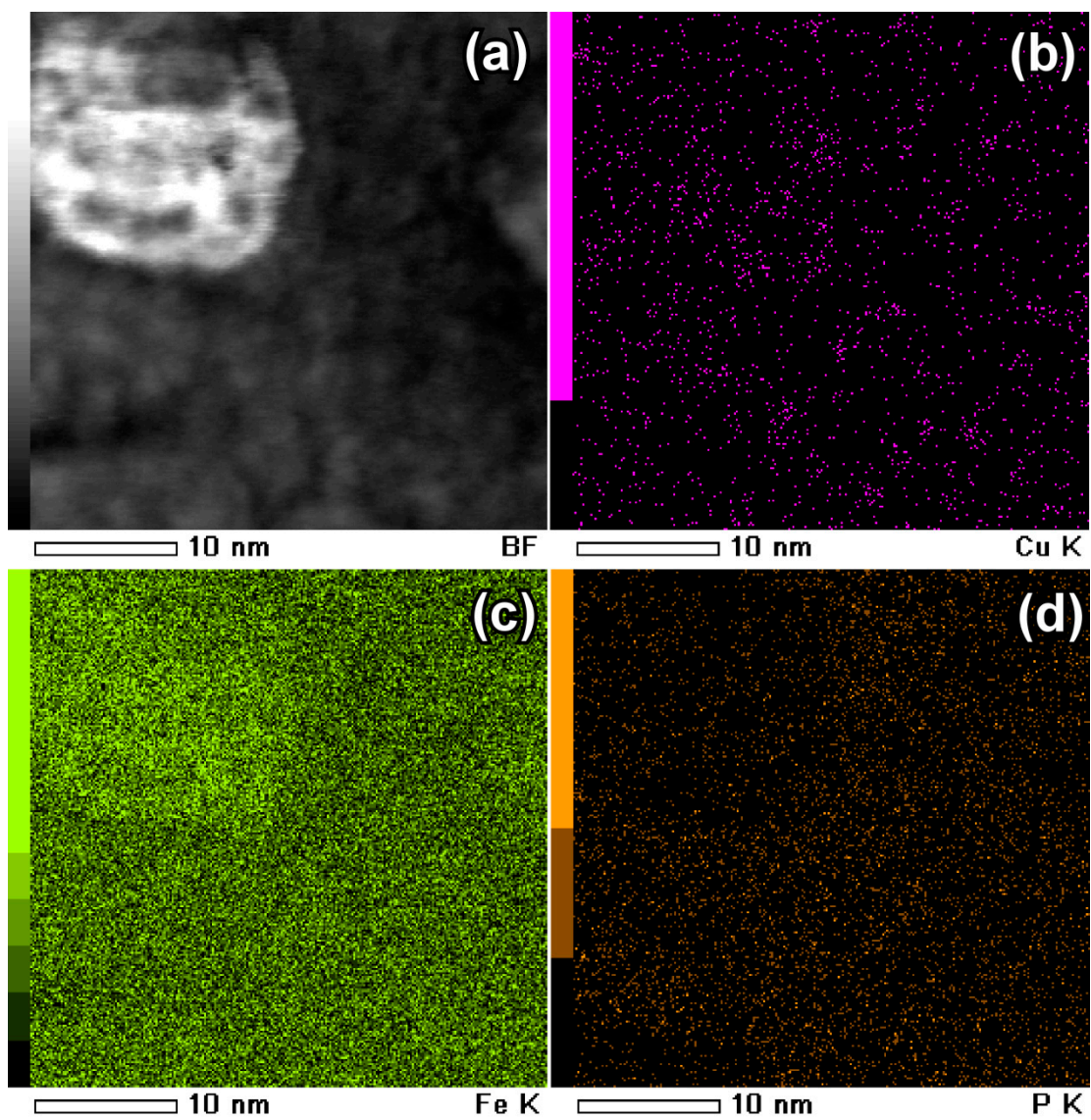


Fig. S1 BFI TEM image (a) and elemental mapping of Cu (b), Fe(c) and P (d) elements in the as-annealed $\text{Fe}_{85.2}\text{B}_{10}\text{P}_4\text{Cu}_{0.8}$ alloys.

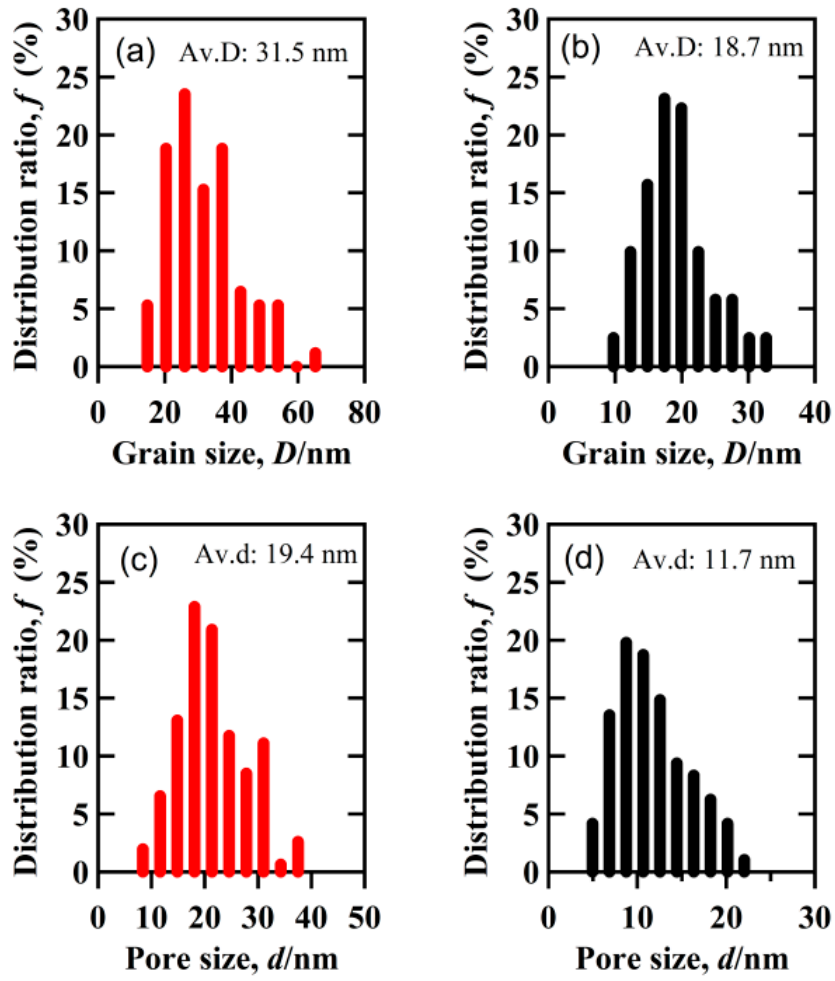


Fig. S2 The distribution ratio of the grain size of a-Fe nanocrystals (a, b) in as-annealed $\text{Fe}_{85.2}\text{B}_{14}\text{Cu}_{0.8}$ and $\text{Fe}_{85.2}\text{B}_{10}\text{P}_4\text{Cu}_{0.8}$ alloys and pore size (c, d) in as-dealloyed $\text{Fe}_{85.2}\text{B}_{14}\text{Cu}_{0.8}$ and $\text{Fe}_{85.2}\text{B}_{10}\text{P}_4\text{Cu}_{0.8}$ alloys.